An in-situ Raman study of the effect of the support for adsorbed iridium-chelates in catalysing oxygen reduction

ELSEVIER

Journal of Electroanalytical Chemistry 406 (1996) 195–202

JOURNAL OF ELECTROANALYTICAL CHEMISTRY

An in-situ Raman study of the effect of the support for adsorbed iridium-chelates in catalysing oxygen reduction

A.L. Bouwkamp-Wijnoltz, B.J. Palys, W. Visscher *, J.A.R. van Veen

Laboratory for Inorganic Chemistry and Catalysis, Eindhoven University of Technology, P.O. Box 513, 5600 MB Eindhoven, Netherlands

Received 17 February 1995; in revised form 24 October 1995

Abstract

In-situ Raman spectroscopy was used to obtain some insight into the mechanism of oxygen reduction at adsorbed layers of iridium-octaethylporphyrin (IrOEP), iridium-tetraphenylporphyrin (IrTPP) and iridium-phthalocyanine (IrPc). The selectivity of adsorbed layers of both porphyrins appears to be very sensitive to the support: on gold only hydrogen peroxide is formed whereas on carbon four-electron reduction is observed. On both supports a peculiar, reversible deactivation occurs at low potentials. IrPc gives hydrogen peroxide on both supports and no deactivation. A previously described single site mechanism is discussed in which only out-of-plane iridium can accomplish the four electron reduction to water and deactivation occurs when the iridium is reduced to its 1 + oxidation state. The results of the in-situ Raman study were generally consistent with this mechanism, but were insufficient to establish it beyond reasonable doubt.

Keywords: Raman spectroscopy; Indium-chelates; Oxygen; Reduction

1. Introduction

Carbon-supported iridium-porphyrins are the only known metal chelates that catalyse the direct four-electron reduction of oxygen in acid [1,2]. In a preceding paper we presented the oxygen reduction activity of carbon-supported iridium-octaethylporphyrin (IrOEP), iridium-tetraphenylporphyrin (IrTPP) and iridium-phthalocyanine (IrPc), before and after heat treatment [1]. It was found that only before heat treatment were the porphyrins selective in forming water. After heat treatment the activity was greatly increased but only hydrogen peroxide was formed, as was the case for IrPc both before and after pyrolysis.

For the adsorbed, non-heat treated (fresh) porphyrins a peculiar, reversible deactivation was also observed at low potentials. A similar behavior was found when the porphyrins were studied for CO oxidation. The results were explained using a single site mechanism, consisting of a geometric part to explain the selectivity variation and a redox part to explain the observed de- and reactivation [1].

In this mechanism the observed four-electron reduction of oxygen was related to a side-on adsorbed oxygen that could be formed if the iridium was out-of-plane with respect to the ligand. For iridium in an in-plane position, only bent adsorption of oxygen should be possible, leading to hydrogen peroxide formation.

The reversible deactivation at low potentials was attributed to the formation of an $Ir(I)–O_2$ species that was irreducible at these potentials. It was also suggested that only an out-of plane iridium could be reduced to the 1 + oxidation state.

The present study involving in-situ resonance Raman spectroscopy was undertaken to try to substantiate the proposed mechanism. Not only carbon-supported layers were studied; for ease of Raman measurement a gold support was employed as well. It turned out, however, that Ir-porphyrins on gold do not show the same selectivity as their carbon-supported counterparts.

2. Experimental

The preparation of the chelates has been described in our previous paper [1]. Pyrolytic graphite and gold were polished with 0.3 and 0.05 μm Al_2O_3 and the electrodes were cleaned using an ultrasonic bath. Irreversibly adsorbed layers onto the freshly polished electrodes were prepared from solutions of the porphyrins in CH_2Cl_2 or of the phthalocyanine in acetone [1].

* Corresponding author.

SSDI 0022-0728(95)04420-5

Rotating ring-disk experiments were performed using equipment as described in Ref. [1]. A.c. voltammetry was performed with equipment provided by the University of Twente [3]. The electrolyte for all electrochemical and in-situ experiments was 0.5 M H_2SO_4.

Raman spectra were recorded with a Confocal Raman microspectrometer [4]. The confocal detection of scattered light restricts the effective measuring volume to roughly 1 μm^3 and suppresses the background signals of the electrolyte and window of the electrochemical cell. Laser power at the sample was 2 mW in all measurements. The 514.5 nm line of the argon ion laser was used for excitation of the porphyrin spectra. The phthalocyanine spectra were measured with the 660 nm line of a dye laser (Spectra Physics model 375B operating with DCM dye). The equipment used for the in-situ electrochemical experiments has been described in a previous paper [5]. The reference electrode, a mercury-sulphate electrode (MSE), was connected to the working electrode via a liquid bridge. Potentials will be given with respect to the RHE, taking MSE as 0.65 V vs. RHE.

3. Results

3.1. Voltammetry

The oxygen reduction of the irreversibly adsorbed iridium-chelates on gold is shown in Fig. 1. A peculiar deactivation at low potentials is present, similar to the behavior found for the adsorbed layers on carbon (Fig. 2) [1]. However, a remarkable change in selectivity with

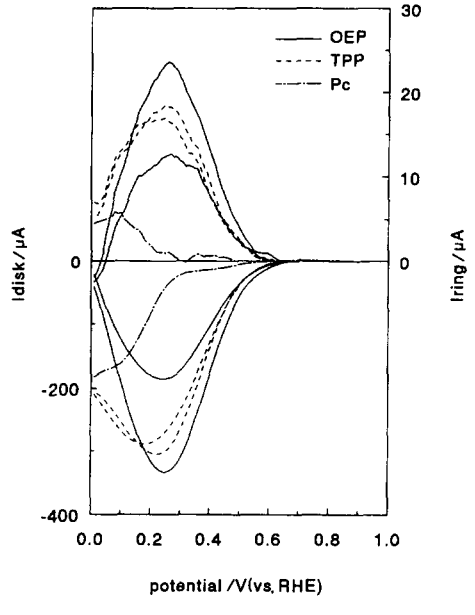

Fig. 1. Oxygen reduction at irreversibly adsorbed iridium-chelates on Au. The currents are corrected for the oxygen reduction at gold. RRDE, 0.5 M H_2SO_4, 16 rev s^{-1}, 10 mV s^{-1}.

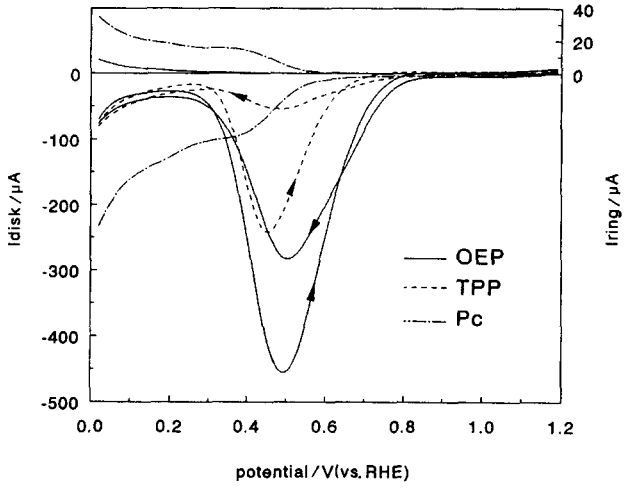

Fig. 2. Oxygen reduction at irreversibly adsorbed iridium-chelates on Cp. RRDE, 0.5 M H_2SO_4, 16 rev s^{-1}, 10 mV s^{-1}.

respect to the carbon support is observed: only hydrogen peroxide is formed, instead of only water! On both supports the IrOEP and IrTPP behave similarly: on carbon only water is formed, on gold only hydrogen peroxide, whereas in both cases the deactivation is present. However, at IrPc only hydrogen peroxide is formed, regardless of the support, and no deactivation is present in either case.

It should be noted that oxygen reduction activity is found only in the case of irreversibly adsorbed layers of iridium-chelates, which are always monolayers on gold. For multilayers, obtained by applying solutions onto the electrode and subsequent evaporation of the solvent, no activity is found.

The a.c. cyclic voltammograms of IrOEP on Cp and on Au in the absence of oxygen are shown in Fig. 3. In both cases a redox transition is observed that is likely to involve the iridium, at about 0.4 and 0.3 V vs. RHE respectively. The wave that is observed at 0.7 V vs. RHE in the gold case (negative scan) is also present in the absence of an adsorbed layer and is ascribed to gold-oxide reduction.

3.2. Raman spectroscopy

The Raman and IR spectra of IrOEP powder are given in Fig. 4. Most of the Raman and IR bands appear to occur at approximately the same position (≤ 20 cm^{-1}) as those observed for NiOEP [6–8]. Therefore, we use the NiOEP data [6–10] for band assignment. Table 1 collects the assignments of the Raman bands. The Raman and IR spectra are complementary, i.e. there are no bands which occur in both Raman and IR, except at 964 and 1276 cm^{-1}. These bands involve large contributions from outer Cβ atoms and from ethyl groups. Therefore, it is very likely that the IrOEP inner macrocycle is flat and has a D4h symmetry. This conclusion agrees with X-ray diffraction data [11,12]: in the IrOEP powder the iridium has two

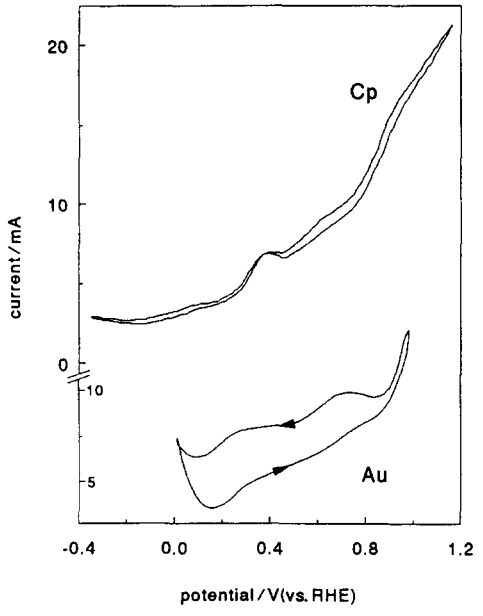

Fig. 3. A.c. voltammogram of IrOEP irreversibly adsorbed on Cp and Au. N_2-saturated 0.5 M H_2SO_4, 50 mV s^{-1}, 300 Hz, 50 mV amplitude.

axial ligands and is in an octahedral environment and an in-plane position with the ligand.

The Raman spectra of IrOEP, adsorbed on Au and Cp, and of IrOEP powder, are given in Fig. 5. The three spectra are very similar, indicating that the symmetry has not been strongly changed. The ν14 band (1126 cm^{-1}) and ν30 band (1165 cm^{-1}) have increased in intensity on both supports, with respect to the dry powder. The intensity of the ν22 band (1142 cm^{-1}) has decreased upon adsorption. The band at 1466 cm^{-1} (ν28) largely disappears upon adsorption. The intensity of the ν7 band (676 cm^{-1}) varies slightly. The peaks in the region 1110–1180 cm^{-1} and the ν28 band all involve pyrrole or macrocycle contributions, so it was assumed that since these bands are most strongly influenced, the pyrroles and/or the macrocycle as a whole are affected by the adsorption. It is thus very likely that, at both Cp and Au, the IrOEP is adsorbed parallel to the surface and remains flat after adsorption.

Table 1
Peak assignment for IrOEP Raman spectrum

Peak position/ cm^{-1}	Assignment; symmetry (PED/%)	Ref.
676 [a]	ν7 A1g; $\delta C\beta C\alpha N\alpha$ (20) + $\nu C\alpha C\beta$ (19)	[6]
	ν7 A1g; $\nu C\alpha N$ (15) + $\delta C\alpha CmC\alpha$ (18) + $\delta C\alpha Cm$ (13)	[7]
758	ν15 B1g; $\nu C\beta Et$ (25) + $\nu C\alpha C\beta$ (20)	[6]
	ν16 B1g; $\delta C\alpha NC\alpha$ (14) + $\nu C\beta Et$ (14)	[6]
784	ν6 A1g; $\delta C\alpha CmC\alpha$ (36) + $\nu C\alpha N$ (27)	[6]
919	ν32 B2g; $\delta C\beta Et$ (50) + $\delta C\alpha Cm$ (22)	[7]
964 [b]	ν46 Eu; $\nu C\beta Et$ (20) + $\delta C\alpha Cm$ (17)	[6]
	ν32 + ν35	[9]
1026	ν5 A1g; $\nu C\beta Et$ (38) + $\nu C\alpha C\beta$ (23)	[6]
1126	ν14 B1g; $\nu C\alpha C\beta$ (31) + $\nu C\beta Et$ (30)	[6]
1142	ν22 A2g; $\nu C\alpha N$ (37) + $\nu C\beta Et$ (26)	[6]
1165	ν30 B2g; $\nu C\beta Et$ (49) + $\nu C\alpha N$ (28)	[6]
1223	ν13 B1g; δCmH (67) + $\nu C\alpha C\beta$ (22)	[6]
1276 [b]	CH_2 twist; E; $\delta C\beta C1H$ (31) + $\delta CetCetH$ (36) ν15 + ν33	[6] [9]
1321	ν21 A2g; δCmH (53) + $\nu C\alpha C\beta$ (18)	[6]
	ν12 B1g; $\nu C\alpha N$ (63) + $\nu C\alpha C\beta$ (13)	
1367	ν20 A2g; $\nu C\alpha N$ (29) + $\nu C\beta Et$ (24)	[6]
1391 [c]	ν4 A1g; $\nu C\alpha N$ (53) + $\delta C\alpha Cm$ (21)	[6]
1408	ν29 B2g; $\nu C\alpha C\beta$ (47) + $\nu C\beta Et$ (26)	[6]
1466	ν28 B2g; $\nu C\alpha Cm$ (52) + $\nu C\alpha C\beta$ (21)	[6]
1559 [c,d]	ν11 B1g; $\nu C\beta C\beta$ (57) + $\nu C\beta Et$ (16)	[6]
1579 [a]	ν2 A1g; $\nu C\beta C\beta$ (60) + $\nu C\beta Et$ (19)	[6]
	ν19 A2g; $\nu C\alpha Cm$ (67) + $\nu C\alpha C\beta$ (18)	
1624 [c]	ν10 B1g; $\nu C\alpha Cm$ (49) + $\nu C\alpha C\beta$ (17)	[6]

νi, skeletal mode; ν, stretching; δ, bending in-plane. [a] Structure sensitive [6]. [b] Also in IR spectrum. [c] Oxidation state marker [6,10]. [d] Axial ligand sensitive [6,10].

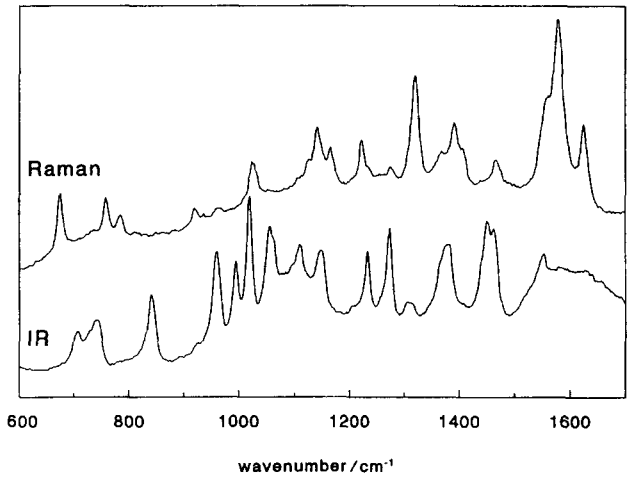

Fig. 4. Resonance Raman (ex-situ, 514.5 nm excitation) and IR (KBr tablet) spectrum of IrOEP.

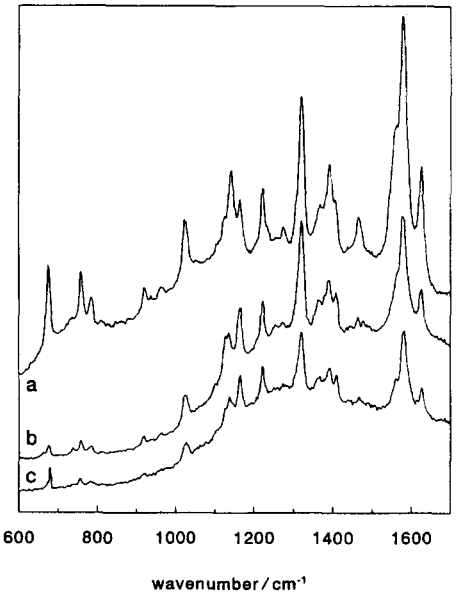

Fig. 5. Raman spectra of different adsorbed layers of IrOEP. a, powder; b, Au; c, Cp.

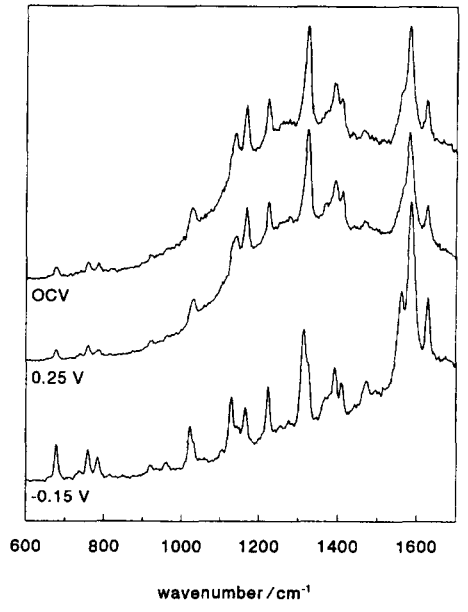

Fig. 6. In-situ Raman spectra of IrOEP adsorbed on gold, air-saturated 0.5 M H_2SO_4.

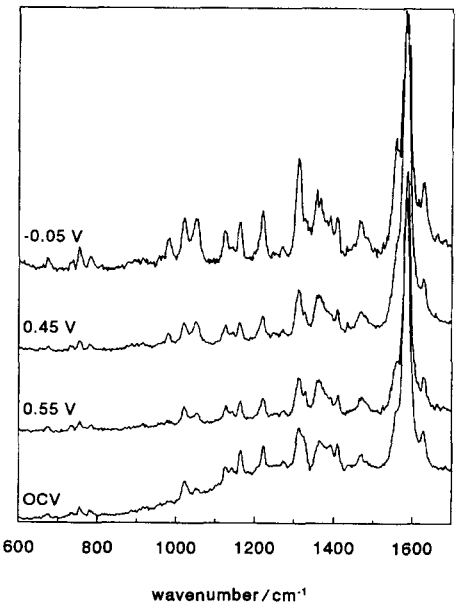

Fig. 7. In-situ Raman spectra of IrOEP adsorbed on Cp, air-saturated 0.5 M H_2SO_4.

The in-situ spectra of IrOEP adsorbed on gold in contact with air-saturated 0.5 M H_2SO_4 are given in Fig. 6 for various potentials. The open circuit voltage (OCV) value was close to 0.7 V. The band at 1364 cm^{-1} (ν20) largely disappears upon contacting the electrode with 0.5 M H_2SO_4 (cf. Fig. 5). Decreasing the electrode potential causes changes in the relative intensities of the oxidation state marker bands at 1391 cm^{-1} (ν4), 1559 cm^{-1} (ν11) and 1624 cm^{-1} (ν10) and a change in the bands between 1100 and 1180 cm^{-1}. Also, a new band at 1311 cm^{-1} becomes visible in the spectrum (possibly at the expense of the band at 1321 cm^{-1} (ν21 or ν12)) and the bands at 1465 cm^{-1} (ν28) and at 676–784 cm^{-1} become more prominent.

The in-situ spectra of adsorbed IrOEP on Cp in contact with air-saturated 0.5 M H_2SO_4 are given in Fig. 7. The spectra are corrected for the Cp spectrum, which has a broad band at around 1300 cm^{-1} and a strong band at 1590 cm^{-1}. The spectra are therefore not very reliable in this region. The band at 1311 cm^{-1} appears in the spectrum already at OCV (0.65 V) and also the ν28 band (1466 cm^{-1}) is again clearly visible. Cathodic polarization of IrOEP on Cp causes different changes in the Raman spectrum as compared with the gold electrode. In Fig. 7 the spectrum at −0.05 V is given, but the spectra between 0.35 and −0.05 V were identical. New features at 980 cm^{-1} and 1050 cm^{-1} are observed, that increase with increasing polarisation. At −0.05 V the 1320 cm^{-1} band has largely disappeared, but as in the gold case the bands at 1559 and 1624 cm^{-1} have increased in intensity. The band at 676 cm^{-1} may be smaller during oxygen reduction (0.55 and 0.45 V) than at OCV and for the deactivated electrode (−0.05 V).

The in-situ spectra of IrTPP adsorbed on Cp and gold in contact with air-saturated 0.5 M H_2SO_4 are given in Figs. 8 and 9. No detailed analysis has been made of the IrTPP Raman spectrum, not only because much fewer comparative data are available in the literature, but also because its quality was not very high. Upon potential cycling only small changes are observed for both Cp and gold.

The in-situ spectrum of IrPc adsorbed on Cp in contact with air-saturated 0.5 M H_2SO_4 is given Fig. 10. The spectrum indicates a D4h symmetry [13], and therefore an

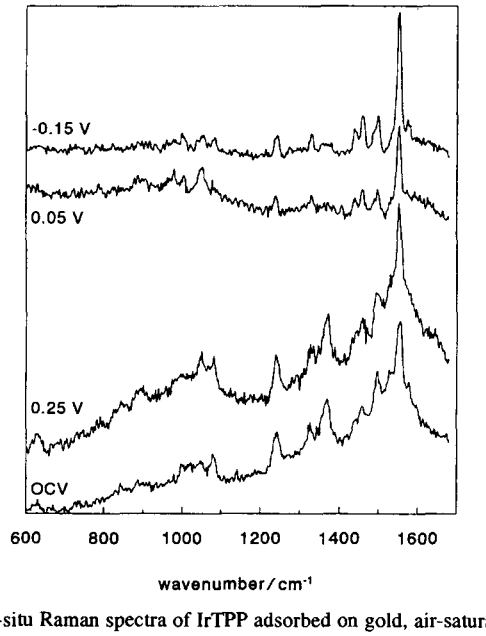

Fig. 8. In-situ Raman spectra of IrTPP adsorbed on gold, air-saturated 0.5 M H_2SO_4.

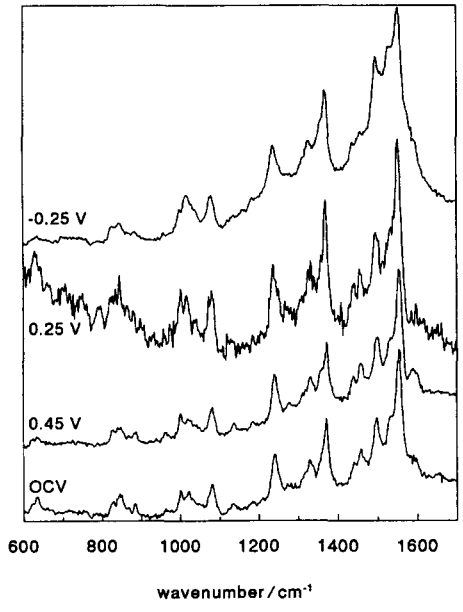

Fig. 9. In-situ Raman spectra of IrTPP adsorbed on Cp, air-saturated 0.5 M H_2SO_4.

in-plane iridium. This is in accordance with the early findings of Keen [14]. Upon potential cycling the symmetry does not change and no conspicuous changes are visible in the spectrum.

Since Raman spectra are taken from monolayers, a SERS effect might contribute (together with the resonance effect) to the enhancement of the Raman signal. However, it is not known how important the SERS contribution might be. Neither the gold nor the pyrolytic graphite surfaces were electrochemically activated before the Raman measurements. In general, such an activation usually enlarges the SERS enhancement factor from 10^2 to 10^6 [15]. Consequently, the SERS enhancement factor in this case will be 10^2 rather than 10^6, while the resonance enhancement reaches at least 10^3. Moreover, no typical SERS dependence between the total spectral intensity and the electrode potential is observed. The potential-dependent changes in the Raman spectrum occur exclusively in the range where oxygen reduction is observed. Therefore, the Raman measurements will be discussed as being the result of oxygen reduction-induced changes.

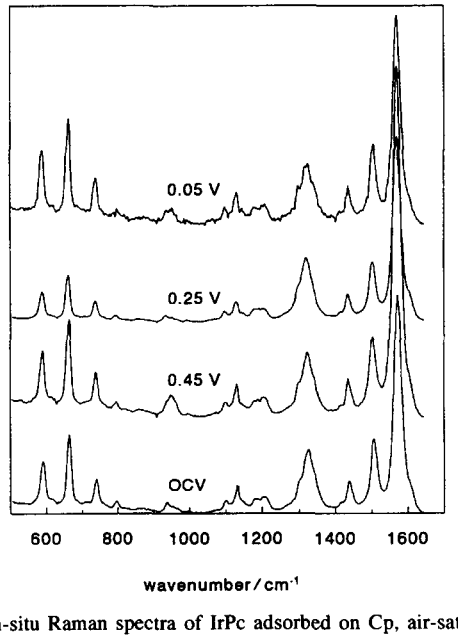

Fig. 10. In-situ Raman spectra of IrPc adsorbed on Cp, air-saturated 0.5 M H_2SO_4.

4. Discussion

Carbon-supported iridium-porphyrins are the only known mono-metal chelates that catalyse the direct four-electron reduction in acid [1,2]. It is, however, remarkable that the selectivity of these chelates in oxygen reduction is so strongly influenced by the support. This observation is also briefly mentioned by Collman et al. [16]. One can ask why only the selectivity is influenced, since the same activation–deactivation phenomena are present on both supports.

Collman and coworkers [2,16] have proposed a dual site mechanism to explain the four-electron reduction of oxygen at IrOEP|Cp. In his view, the active species is the dimer $(IrOEP)_2$, which reacts with oxygen to form a μ-peroxo species which is then reduced to water and the original dimer, thus closing the catalytic cycle. The $(IrOEP)_2$ dimer could not actually be produced through bulk electrolysis (it does exist; it can be prepared by oxidation of IrOEP–H [17]), but Collman interpreted his own finding that IrTPP is totally inactive (!) to mean that the TPP ligand is too sterically hindered to form the dimer required to start the catalytic cycle. Our finding that IrTPP does behave in the same way as IrOEP already invalidates this argument, but the dimer idea is suspect on other grounds as well.

— The facts that IrOEP and IrTPP produce water when adsorbed on Cp and hydrogen peroxide when adsorbed on Au, and that the sterically unhindered IrPc always produces hydrogen peroxide, are difficult to reconcile with the idea that oxygen reduction necessarily takes place via a dimer.

— The fact that CO oxidation takes place at iridium porphyrins in the same potential range as that in which oxygen reduction occurs [1], taking into account that this reaction starts with the adsorption of CO on an Ir(III) single site [18,19], mitigates against the assumption that a dimer should be the active species.

Furthermore, it is noted that aged porphyrins (IrOEP and IrTPP) drop drastically in oxygen reduction activity and produce only hydrogen peroxide, even when supported on carbon. For the aged porphyrins also no deactivation at low potentials is present.

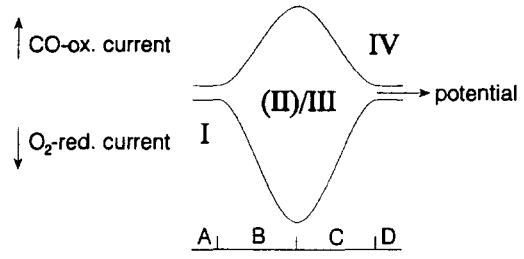

Scheme 1.

It is realized that the initial urge on seeing 100% selectivity to water is to assume a dual site mechanism, usually in the form of an initial dimerization of the chelate under study, a recent example being Lever and coworkers' work on adsorbed RhPc–Cl [20]. Here, however, we should like to discuss our previously proposed single site mechanism [1] for oxygen reduction at iridium-chelates, consisting of a geometric part to explain the observed selectivity variation and a redox part to explain the observed de- and reactivation.

In the proposed single site mechanism the iridium is supposed to switch valency rather easily. Schematically, the different oxidation state regions of the iridium are as shown in Scheme 1 [1].

With a.c. voltammetry a redox transition for IrOEP on both Cp and gold is found, approximately at the potential where the oxygen reduction is at its maximum. It is to be noted that in our previous paper no redox transition could be observed with cyclic voltammetry [1]. Also, Collman and Kim found a redox transition at this position [2]. The redox transition may be attributed to the Ir^{III}/Ir^{I} transition. This transition is also the only metal-based one observed for dissolved IrOEP [11].

The in-situ Raman spectra of IrOEP on both gold and Cp show, at low potentials, region A, as compared with the spectra at other potentials, an increase in the relative intensities of the bands at 1559 (ν11) and 1624 (ν10) cm^{-1}, which are oxidation state markers in the case of iron-porphrins [6,10]. Since the ν11 vibration is also sensitive to the binding of an axial ligand and the band at 676 cm^{-1} (ν7) also increases, this may indicate that the Ir coordination has returned to octahedral as in the as-prepared complex (cf. the powder spectrum, Fig. 4). This is not inconsistent with our proposed irreducible $Ir(I)–O_2$ species, but some form of dimer cannot be rigorously excluded. However, in our case the dimer would be at most the deactivated species, not the active form of the catalyst.

The observed selectivity variance has been related to the configuration in which oxygen can adsorb [1]: side-on adsorbed oxygen would lead to water formation and was related to an out-of-plane iridium. Bent adsorbed oxygen could only lead to hydrogen peroxide formation and was assumed when the iridium was in an in-plane position with respect to the ligand plane.

For the pure IrOEP it was concluded that the metal chelate is flat, i.e. that the iridium atom is positioned in the macrocycle. The similarity of the Raman spectra of pure IrOEP and IrOEP adsorbed on gold suggest that on gold the IrOEP also remains flat. The in-situ spectra show that this situation still holds at OCV conditions and at potentials down to that at which maximum activity is observed, in that there is no indication for a lowering of the molecular symmetry (i.e. no new bands or broadening of the bands is observed). For this reason we suppose that the IrOEP molecule adsorbed on gold remains flat during the catalytic reaction. For adsorbed IrPc a similar conclusion can be reached, since the in-situ Raman spectrum indicates a D4h symmetry and it does not change significantly during oxygen reduction (Fig. 10). So far, so good.

Now, if indeed the position of the iridium determines the selectivity, it is rather remarkable that the selectivity of adsorbed IrOEP can be completely changed just by exchanging gold for Cp. But, by influencing the core size of the macrocycle, the position of the iridium with respect to the macrocycle ring might be varied. It has been found for NiOEP, by Brennan et al. [21], that an increase in π–π interaction causes a decrease in π charge density in the porphyrin ring. This decrease in π change causes a contraction of the porphyrinato core. The bands that reflect this are the ν10 (1624 cm^{-1}), ν19 (1579 cm^{-1}) and ν3 (not visible in our spectrum) bands and the oxidation state marker band ν4 (1391 cm^{-1}) [21,22]. These are therefore called core size markers, but ν10 and ν4 are also sensitive to the oxidation state of the metal ion. The ν21 (1321 cm^{-1}), ν29 (1408 cm^{-1}) and ν11 (1559 cm^{-1}) bands sometimes also reflect differences in core size [21]. Thus, a difference in π–π interaction between IrOEP|Cp and IrOEP|Au could be at the origin of the observed differences in selectivity of the two systems. Of the six core size marker bands mentioned above, four have rather similar intensities in the in-situ Raman spectra of the two systems, but the 1321 cm^{-1} band is much less prominent in the IrOEP|Cp spectrum than in that of IrOEP|Au, and the 1391 cm^{-1} band is prominent in the Au case but virtually absent in the Cp one. This is qualitative evidence that the core sizes may indeed differ in the two cases, resulting in an in-plane Ir for the Au case and an out-of-plane Ir for its Cp counterpart.

Even if the change in core size is real for IrOEP, with its implication that there is a large difference in π–π interaction between the macrocycle and the Cp or Au support, such an effect should perhaps be expected to be much less for the sterically hindered IrTPP, but here the same selectivity variation is observed. A small indication, however, that the coordination of the iridium during oxygen reduction for IrOEP|Cp is indeed square pyramidal is provided by the ν7 band (676 cm^{-1}) [6]. During oxygen reduction this band is almost absent, whereas at Au it is still clearly visible, indicating an octahedral or square planar environment for the iridium in the latter system.

It might have been expected that a few new bands would appear in the Raman spectrum when the Ir atom is out of the molecular plane rather than in it. After all, the molecular symmetry changes then from D4h to C4v, and in consequence, IR active A2u modes become totally symmetrical and are allowed in the resonance Raman spectrum. However, since there are only very few A2u bands in the IR spectrum [23], it is not too surprising that no new bands are actually observed in Raman. The modes of Eu symmetry only become possible when the molecule loses its four-fold symmetry axis.

During potential cycling some changes occur between 1110 and 1180 cm^{-1} for both IrOEP|Cp and IrOEP|Au. Also, the new bands at 1050 and 980 cm^{-1} for IrOEP|Cp are remarkable. The bands at 1110–1180 cm^{-1} can be ascribed to pyrrole or macrocycle vibrations, and it is not unlikely that these are influenced when oxygen reduction takes place and the electron density on the iridium changes. The origin of the bands at 1050 and 980 cm^{-1}, however, is obscure.

We have explored the possibility that oxygen bands are involved. Watanabe et al. [24] found two bands for iron-porphyrins that could be attributed to end-on adsorbed oxygen (νO–O 1190 cm^{-1}) and side-on adsorbed oxygen (νO–O 1104 cm^{-1}). In this IR study at 15 K the end-on band was much more intense than the side-on band. Both bands disappeared upon heating and were no longer present at room temperature.

If we were to assign the band at 1050 for IrOEP|Cp to side-on adsorbed oxygen, one would expect the end-on oxygen band for IrOEP|Au at approximately 1140 cm^{-1}. Indeed, in this region potential-induced changes are observed, but these are similar for both Cp and Au. Assignment of 980 cm^{-1} to the side-on νO–O band leads to a similar conclusion, no $\sim$ 1070 cm^{-1} band being present in the IrOEP|Au spectrum.

Again, we cannot rigorously exclude the possibility that a dual site mechanism is involved: the two new bands could point to the formation of a peroxo complex, since for peroxo dimers two (oxygen involved) vibrations are observed [25]. However, similar bands for IrTPP are absent, thus weakening the dual site mechanism proposal.

So, it is unlikely that the bands at 1050 and 980 cm^{-1} can be ascribed to vibrations involving oxygen. It cannot be excluded that the 980 cm^{-1} band is associated with a sulfate vibration, but one could question why this vibration is, in this case, not present in all spectra. At very low potentials one hardly expects a negatively charged species to coordinate to the electrode surface. Furthermore, since the Raman spectra are resonance-enhanced, a sulfate vibration should, if visible, have only a very small intensity.

It has been mentioned by Kitagawa et al. [26] that a band at 980–1000 cm^{-1} becomes visible in the Raman spectrum of a metal-substituted OEP upon ring deformation. If this is correct, the 980 cm^{-1} band can be assigned to the 1050 cm^{-1} band and could originate from an IR active mode that becomes visible in the spectrum as a result of the decreasing symmetry.

It is clear from the above the none of the changes observed in the Raman spectra during O_2 reduction can readily be ascribed to an Ir–O_2 complex. This could, of course, very well be due to the low stability of such a complex. However, it is worth emphasizing that none of the observations and possible explanations is in conflict with the proposed single site mechanism, consisting of a redox part and a geometric part.

5. Conclusions

At IrOEP as well as at IrTPP adsorbed on gold, reduction of oxygen leads to hydrogen peroxide formation. However, for the same porphyrins adsorbed on pyrolytic graphite, four-electron reduction is observed. A peculiar de- and reactivation process occurs for both adsorbed layers at low potentials.

The oxygen reduction on iridium sites can be explained with a single site mechanism, taking into account redox transitions to explain the catalytic cycle as well as the de- and reactivation processes where iridium is considered to be active only in its II and III valence states, but inactive in its IV and I valence states, cf. Scheme 1, and a geometrical description to explain the observed selectivity variation. The position of the iridium is considered to determine whether oxygen–oxygen bond cleavage is possible: for the out-of-plane iridium in porphyrins side-on adsorption of oxygen and water formation occurs, whereas for the in-plane iridium such as in the phthalocyanine only bent adsorption and hydrogen peroxide formation is found.

The results of our in-situ Raman study are generally consistent with the above explanation, but are insufficiently clear-cut to actually establish it beyond reasonable doubt.

Acknowledgement

The authors want to warmly thank Dr. G.J. Puppels (University of Twente) for allowing them to use his Raman equipment.

References

[1] A.L. Bouwkamp-Wijnoltz, W. Visscher and J.A.R. van Veen, Electrochim. Acta, 39 (1994) 1641.
[2] J.P. Collman and K. Kim, J. Am. Chem. Soc., 108 (1986) 7847.
[3] D. van den Ham, C. Hinnen, G. Magner and M. Savy, J. Phys. Chem., 91 (1987) 431.
[4] G.J. Puppels, W. Colier, J.H.F. Olminkhof, C. Otto, F.F.M. de Mul and J. Greve, J. Raman Spectrocs., 22 (1991) 217.
[5] B.J. Palys, G.J. Puppels, D. van den Ham and D. Feil, J. Electroanal. Chem., 326 (1992) 105.

[6] M. Abe, T. Kitagawa and Y. Kyogoku, J. Chem. Phys., 69 (1978) 4526.
[7] X.Y. Li, R.S. Czernuszewicz, J.R. Kincaid, P. Stein and T.G. Spiro, J. Phys. Chem., 94 (1990) 47.
[8] X.Y. Li, R.S. Czernuszewicz, J.R. Kincaid and T.G. Spiro, J. Am. Chem. Soc., 111 (1989) 7012.
[9] T. Kitagawa, M. Abe and H. Ogoshi, J. Chem. Phys., 69 (1978) 4516.
[10] T.G. Spiro and T.C. Strekas, J. Am. Chem. Soc., 96 (1974) 338.
[11] C. Swistak, J.L. Cornillon, J.E. Anderson and K.M. Kadish, Organometallics, 6 (1987) 2146.
[12] K.S. Chan, X.M. Chen and T.C.W. Mak, Polyhedron, 11 (1992) 2703.
[13] R. Aroca, Z.Q. Zeng and J. Mink, J. Phys. Chem. Solids, 51 (1990) 135.
[14] I.M. Keen, Platinum Met. Rev., 8 (1964) 143.
[15] R.K. Chang and T. Furtak (Eds.), Surface Enhanced Raman Scattering, Plenum Press, New York, 1982.
[16] J.P. Collman, P.S. Wagenknecht and J.E. Hutchison, Angew. Chem., 106 (1994) 1620.
[17] K.S. Chan and Y.B. Leung, Inorg. Chem., 33 (1994) 3197.
[18] J.F. van Baar, J.A.R. van Veen and N. de Wit, Electrochim. Acta, 27 (1982) 57.
[19] J.F. van Baar, J.A.R. van Veen, J.M. van der Eijk, Th.J. Peters and N. de Wit, Electrochim. Acta, 27 (1982) 1315.
[20] Y.H. Tse, P. Seymour, N. Kobayashi, H. Lam, C.C. Leznoff and A.B.P. Lever, Inorg. Chem., 30 (1991) 4453.
[21] T.D. Brennan, W.R. Scheidt and J.A. Shelnutt, J. Am. Chem. Soc., 110 (1988) 3919.
[22] J.A. Shelnutt, C.J. Medforth, M.D. Berber, K.M. Barkigia and K.M. Smith, J. Am. Chem. Soc., 113 (1991) 4077.
[23] A.L. Wijnoltz, Thesis, Eindhoven University of Technology, 1995.
[24] T. Watanabe, T. Ama and K. Nakamoto, J. Phys. Chem., 88 (1984) 440.
[25] K. Nakamoto, Coord. Chem. Rev., 100 (1990) 363.
[26] T. Kitagawa, M. Abe, Y. Kyogoku, H. Ogoshi, E. Watanabe and Z. Yoshida, J. Phys. Chem., 80 (1976) 1181.